Sensors and Materials, Vol. 36, No. 4 (2024) 1377–1387
MYU Tokyo

S & M 3605

Prediction of Flying Height Using Deep Neural Network Based on Particle Swarm Optimization in Hard Disk Drive Manufacturing Process

Worawit Kanjanapruthipong,[1] Pitcha Prasitmeeboon,[2] and Poom Konghuayrob[3*]

[1]Department of Robotics and AI Engineering, School of Engineering, King Mongkut's Institute of Technology Ladkrabang, 1, Soi Chalong Krung 1, Ladkrabang, Bangkok 10520, Thailand
[2]Department of Control Engineering, School of Engineering, King Mongkut's Institute of Technology Ladkrabang, 1, Soi Chalong Krung 1, Ladkrabang, Bangkok 10520, Thailand
[3]Department of Electrical Engineering, School of Engineering, King Mongkut's Institute of Technology Ladkrabang, 1, Soi Chalong Krung 1, Ladkrabang, Bangkok 10520, Thailand

(Received December 26, 2023; accepted March 13, 2024)

Keywords: flying height, deep neural network, particle swarm optimization, hard disk drive, DNNpso, AI

In contemporary hard disk drive (HDD) manufacturing processes, after the assembly of the HDD from the production line, a series of diverse calibration procedures are necessary to ensure standardization. These include capacity calibration, which determines the storage space in terabytes (TB) presently available, and flying height (FH) calibration, which evaluates the distance between the head and the disk by applying electric current to the heater coil element to achieve the desired FH, thus optimizing the writing and reading performance and tailoring it to each HDD. Additionally, electric current is saved in a digital-to-analog converter (DAC) unit for the utilization of a read/write head, while a preamp collaborates with the drive firmware to convert the electric current in the DAC unit to milliwatts. In the present scenario, multiple calibrations of flying heights (FHs), specifically flying height 1 (FH1) and flying height 2 (FH2), are performed. Each FH calibration requires a testing time of approximately 5 h owing to the separation of measurement points into 240 locations across the disk surface, referred to as test zones, with a total of 20 heads. The primary objective of this study is to reduce the testing time by using a combination of deep neural network (DNN) and particle swarm optimization techniques to predict the DAC profiles of FH2 as it approaches FH1, where FH1 is the input for the DNN model.

1. Introduction

In hard disk drive (HDD) manufacturing, the calculation of the flying height (FH) for read/write heads is crucial to ensure efficient and effective read/write operations that are optimized for each HDD. Dakroub *et al.*[(1)] studied the measurement of FH for an HDD by examining the amplitude of the signals used in this process. Schardt *et al.*[(2)] developed a technique for measuring FH, which involves the movement of read/write heads from the inner track to the

*Corresponding author: e-mail: poom.ko@kmitl.ac.th
https://doi.org/10.18494/SAM4825

ISSN 0914-4935
https://myukk.org/

outer track of the disk. Novotny[3] developed a novel technique for characterizing the magnetic amplitude to investigate the spacing between the read/write heads and the high-bandwidth disk during track seeking, head parking, vibrations, and shocks while the HDD is operational. This investigation involved the measurement of magnetic flux densities to assess the magnetic profiles. Juang *et al.*[4] performed a nonlinear modeling of the read/write head, accurately simulating its protrusion, which affects the variation in FH under different environmental conditions. Boettcher *et al.*[5] performed a dynamic FH measurement with feedforward control to optimize variations.

These studies attempted to find methods for obtaining read/write heads with optimal and efficient FH profiles. In this study, we propose a novel approach by combining a deep neural network (DNN) with an enhanced particle swarm optimization (PSO)[6–15] algorithm to find a suitable number of nodes for each hidden layer of the DNN. This innovative approach uses AI techniques, specifically a DNN, in conjunction with improved PSO techniques to predict the digital-to-analog converter (DAC) profiles of flying height 2 (FH2) with optimal performance. By employing this methodology, it is anticipated that the amount of FH measurement and the operation of the read/write head will be significantly reduced. This would result in a highly accelerated FH measurement process while maintaining comparable efficiency to conventional measurement methods. We aim to reduce the production time per unit in the manufacturing line of an HDD, as shown in Fig. 1, and for measuring the DAC profiles for flying height 1 (FH1) and FH2, which currently takes approximately 5 h (Fig. 2). In this way, we can reduce the measurement time of FH2 using an AI-based approach.

2. Experimental Procedure

2.1 Point of interest in FH measurement

The process of measuring the FH of the read/write head involves measuring the protrusion value in the DAC unit, which is from the tip of the read/write head to the position called the target FH at point B in Fig. 3. Distance A refers to the thermal protrusion in the DAC unit, the focus of this study.

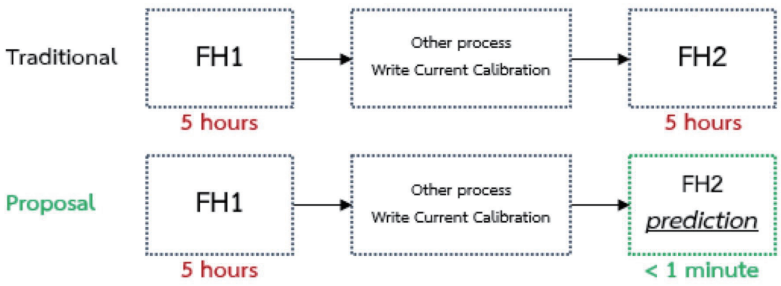

Fig. 1. (Color online) FH measurement process and test time reduction concept for FH2 measurement.

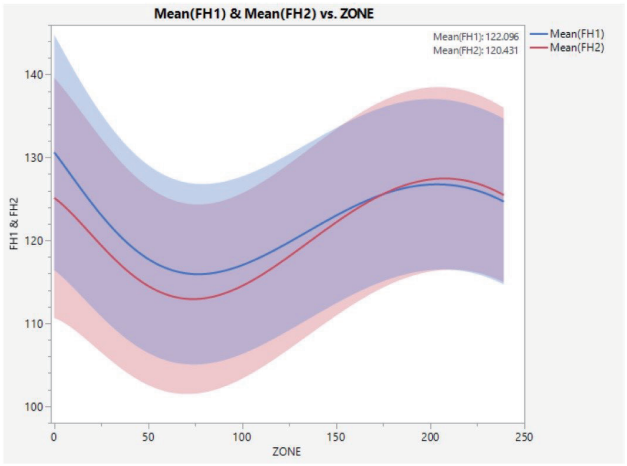

Fig. 2. (Color online) Profile of DAC for FH1 and FH2 measurements.

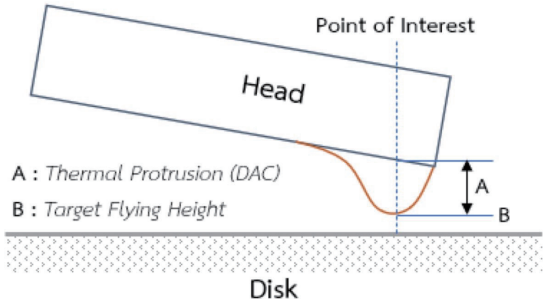

Fig. 3. (Color online) Points of interest in head reading/writing for FH measurement.

2.2 Deep neural network based on particle swarm optimization

In this study, we present a novel method of FH prediction using a DNN combined with an efficiency-enhanced PSO algorithm, called DNNpso. The objective is to find an appropriate and efficient number of nodes in the hidden layers for predicting the FH profile, which is measured in the DAC unit, as shown in Fig. 4.

2.3 Preparation of data and evaluation criterion

Preparing data for training involves utilizing information from 50 HDDs, each comprising 20 read/write heads across 240 zones. Consequently, there is a dataset of 240,000 points (50 × 20 × 240) for training the DNN model. This dataset is partitioned into 80% for training and 20% for validation. The input features for the model include the DAC value for FH1, the head, the zone, the current, and the default current. The output result is the DAC value for FH2, as shown in the

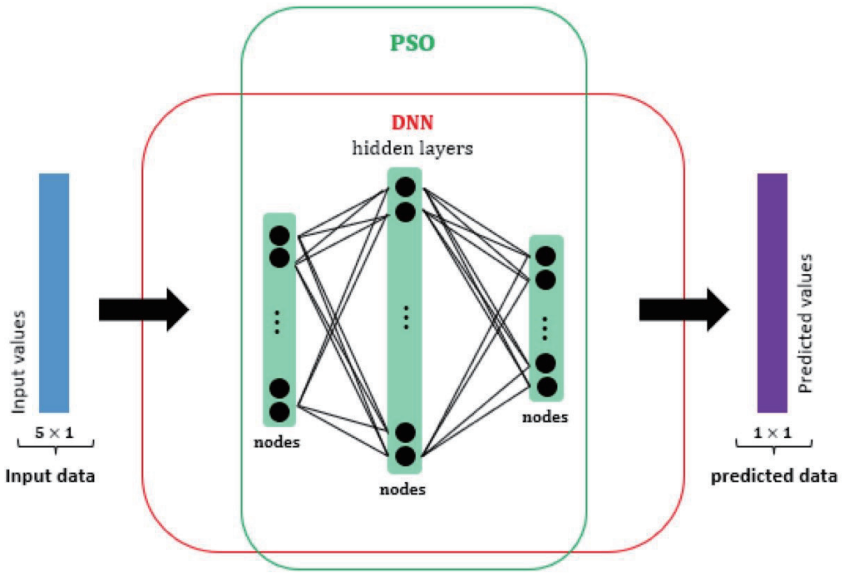

Fig. 4. (Color online) DNNpso architecture.

relationship depicted in Fig. 5. Data input relationships are sequenced using the Bootstrap Forest method, which is based on the Decision Trees method, as shown in Fig. 6. In this study, three hidden layers are utilized in the DNN. PSO is utilized to determine the appropriate number of nodes using Eqs. (1) and (2). Objective functions are defined on the basis of the R^2 metric, as outlined in Eq. (3), derived from the FH measurements of the actual HDD and the values predicted with the model. The DNN model is trained using the mean square error (MSE) as the loss function, represented by Eq. (4). The DNN utilizes the backpropagation algorithm to calculate the derivatives of the error with respect to the weights from the previous iteration, then the weights are adjusted to minimize the error, as depicted in Eq. (5).

Particle swarm optimization (PSO):

$$V_{t+1}^{i} = wV_{t}^{i} + c_1 r_1 \left(pb^{i} - X_{t}^{i} \right) + c_2 r_2 \left(gb - X_{t}^{i} \right) \tag{1}$$

$$X_{t+1}^{i} = X_{t}^{i} + V_{t+1}^{i} \tag{2}$$

Coefficient of determination or R^2:

$$R^2 = 1 - \frac{\sum_{i=1}^{n} \left(y_i - \overline{y}_i \right)^2}{\sum_{i=1}^{n} \left(y_i - \mu \right)^2} \tag{3}$$

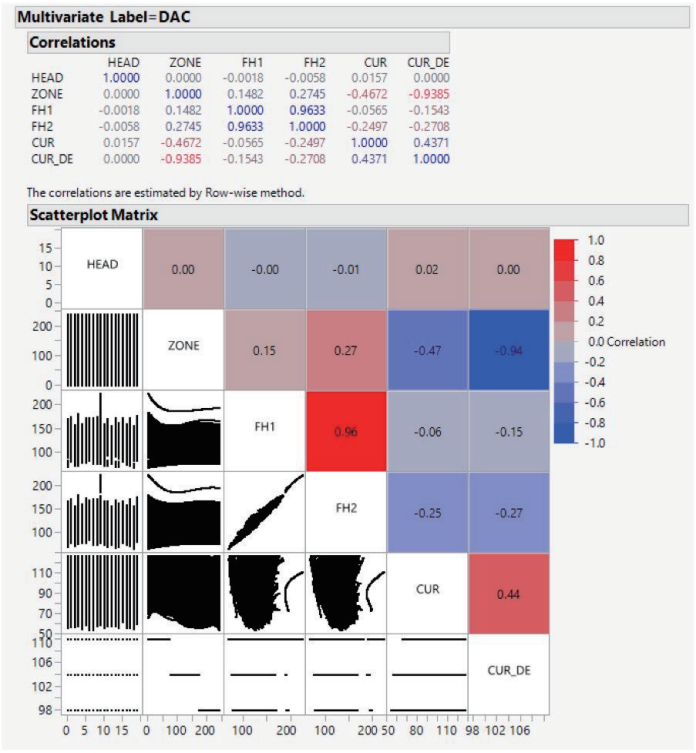

Fig. 5. (Color online) Relationship between input and output.

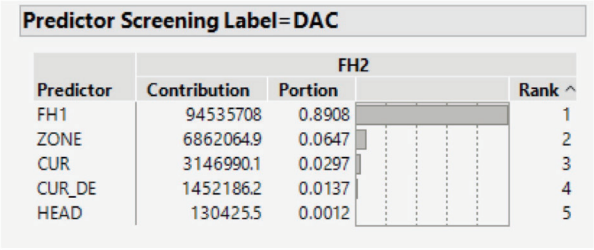

Fig. 6. (Color online) Arrangement of input relationships using Bootstrap Forest method.

Mean square error:

$$MSE = \frac{\sum_{i=1}^{n} \left(y_i - \overline{y}_i \right)^2}{n} \tag{4}$$

Backpropagation algorithm (for DNN):

$$*w_x = w_x - \alpha\left(\frac{\partial error}{\partial w_x}\right) \tag{5}$$

In these equations, y represents true values, $\bar{y}$ denotes predicted values, μ is the mean of the true values, and n is the number of data points in the dataset. Generally, a lower MSE signifies more accurate predictions, namely, the predicted values $\bar{y}$ closely align with the true values. R^2 is a metric for the goodness of fit in regression and ranges between 0 and 1, with a score of 1 indicating perfect prediction and higher values indicating better predictive performance.

The backpropagation algorithm, employed in the training phase of the DNN, involves parameters including w_x and *error*. w_x represents the weights and *error* denotes the error from the previous iteration. The parameter α signifies the learning rate. The algorithm iteratively updates the weights, forwarding them to $*w_x$, during each training cycle.

PSO aims to determine a suitable and efficient number of nodes for the hidden layers in a DNN. In this context, w represents the momentum coefficient, V is the velocity of the particle, X denotes the position of the particle, and *c1* and *c2* are random constants within the range [0, 1]. *pb* (*pbest*) refers to the particle's personal best, which is the highest objective function value the particle has encountered locally, and *gb* (*gbest*) is the highest objective function value encountered globally over all previous iterations. i is the number of iterations and t is the current particle.

3. Results and Discussion

From the experiments conducted with DNNpso, it was observed that the particle swarm group effectively aids in determining a suitable number of nodes for each hidden layer. In this study, a Particle Swarm of 10 was employed and 20 iterations were performed, where the 10 particles attempted to find directions to adjust the number of nodes to align with the objective function, using R^2 as the performance indicator. This process was repeated for 20 iterations, giving a consistent R^2 of ≈ 0.96, as shown in Fig. 7 and Table 1. Furthermore, we attempted to identify the optimal number of iterations for this study. It was observed that after 10 iterations, there was only a marginal improvement in R^2, as shown in Fig. 8. Consequently, we set the number of iterations at 20.

A detailed examination of the experimental results for each particle swarm reveals variations among the swarms. It is observed that a favorable R^2 obtained from DNNpso indicates a strong relationship between the actual FH measurements and the predictions from the 20% validation dataset, as shown in Fig. 9 in which the green-bordered frame indicates the highest R^2 and the best correlation, and therefore the optimal performance of PSO. The distribution of R^2 for each particle swarm is shown in Fig. 10.

After obtaining a satisfactory model, it was saved for future use. The model was then tested using data from 40 HDDs, which were not part of the 80% training or 20% validation group. The

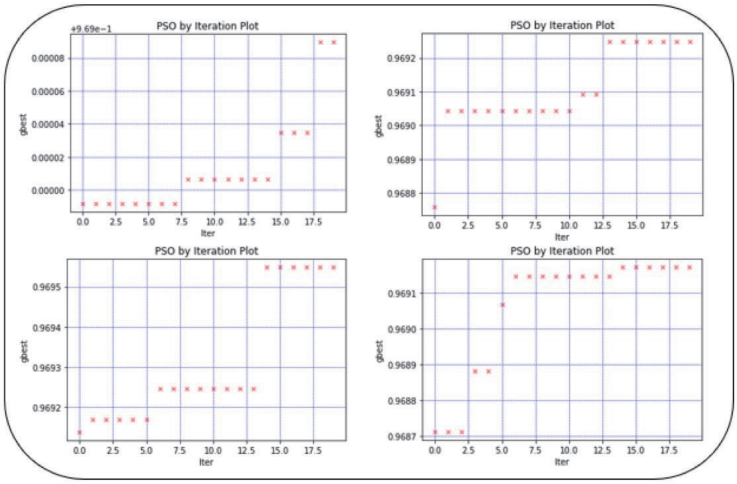

Fig. 7. (Color online) Experimental results of DNNpso with R^2 as the objective function.

Table 1
Experimental results of repeated model training with selected configuration to find the best objective function (R^2).

Run	Iterations	Particle swarm	Epochs (DNN)	*MSE*	R^2	Training time (s)
1	20	10	10	0.000203	0.9690	21.0744
2	20	10	10	0.000200	0.9692	10.0495
3	20	10	10	0.000199	0.9695	26.4638
4	20	10	10	0.000202	0.9691	45.4285

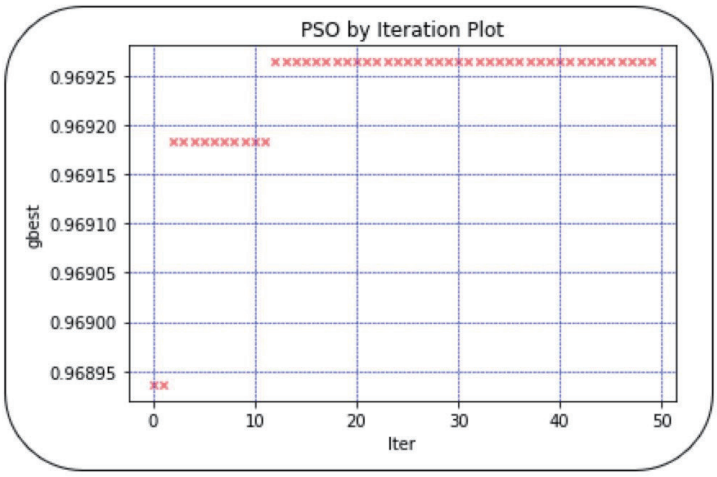

Fig. 8. (Color online) Experimental outcomes of adjusting iterations in DNNpso.

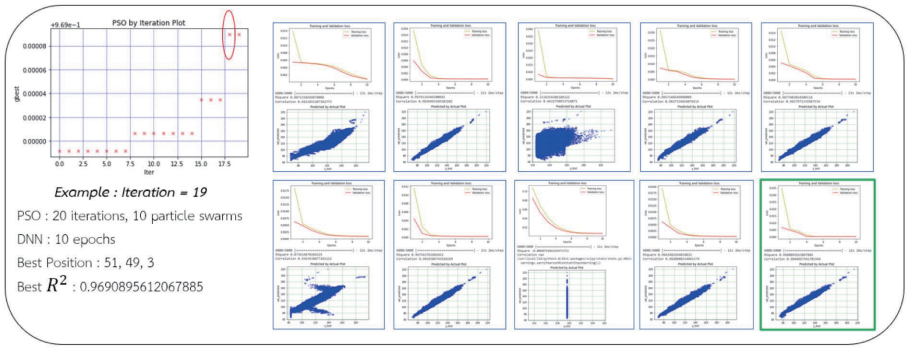

Fig. 9. (Color online) Experimental results of comparative analysis of relationship between number of iterations and R^2 in DNNpso for each particle swarm.

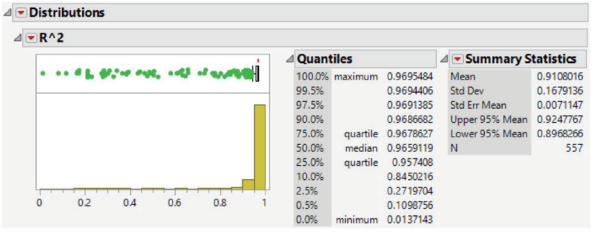

Fig. 10. (Color online) Distribution of R^2 in DNNpso for each particle swarm.

experiments yielded promising results with a correlation of ≈ 0.98 (R^2 ≈ 0.97), as shown in Fig. 11. This value indicates a high accuracy and a strong correlation between the actual FH measurements and the values predicted with the model. The boxplot exhibits uniformity, with a mean value of approximately 120 DAC and a standard deviation of around 12.8, and the cumulative distribution function (CDF) probability [Eq. (6)] was consistent between the actual FH measurements and the corresponding predictions, as shown in Fig. 12.

$$F_x(x) = P(X \le x) = \sum_{x_i < x} P(X = x_i)$$
$$x \in [0, 255], x : DAC \tag{6}$$

Furthermore, the DAC profile, which is a comprehensive representation derived from both actual measurements and predictions, demonstrates a highly satisfactory alignment between the two, as clearly illustrated in Fig. 13. Moreover, DAC profiles are dissected for each read/write head. The experimental results exhibit consistently good performance, as depicted in Fig. 14. Detailed statistical values such as mean and standard deviation can be extracted from Fig. 12.

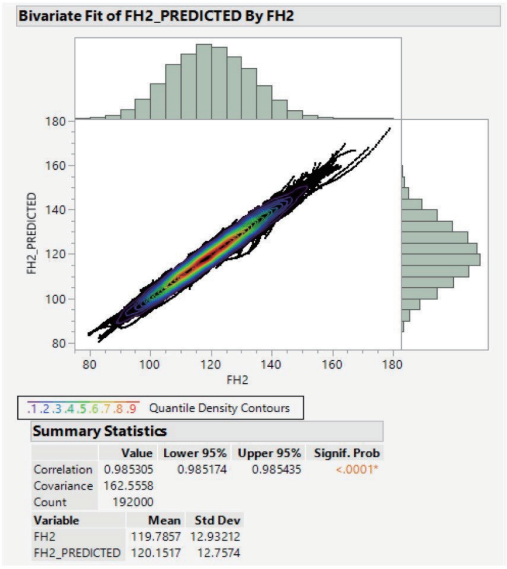

Fig. 11. (Color online) Correlation values obtained from actual measurements and predictions using the new HDD group.

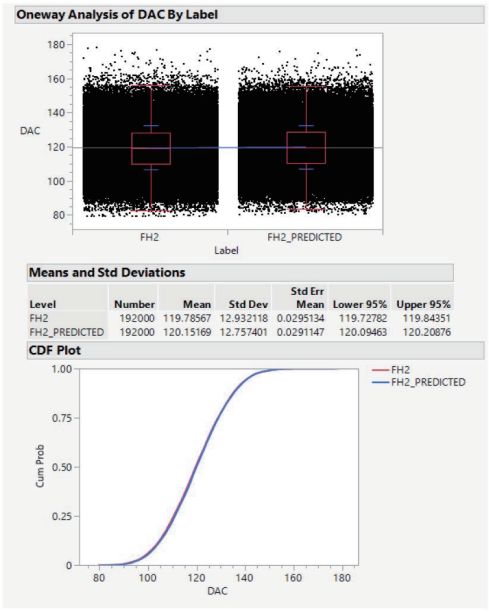

Fig. 12. (Color online) Boxplot and CDF obtained from actual measurements and predictions using the new HDD group.

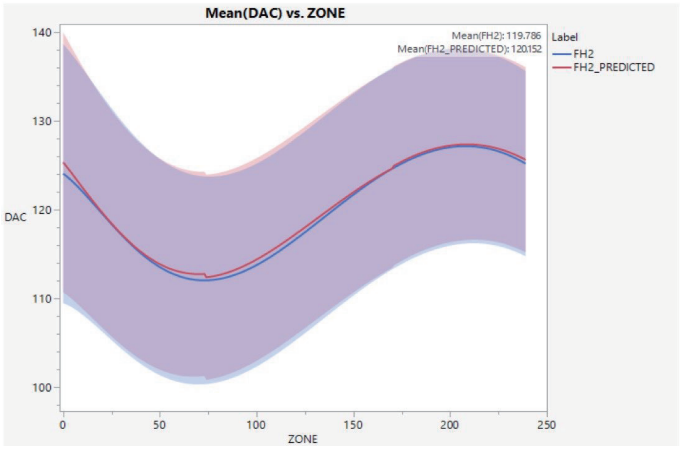

Fig. 13. (Color online) DAC profile resulting from the actual measurements and predictions of FH2 from the new HDD group.

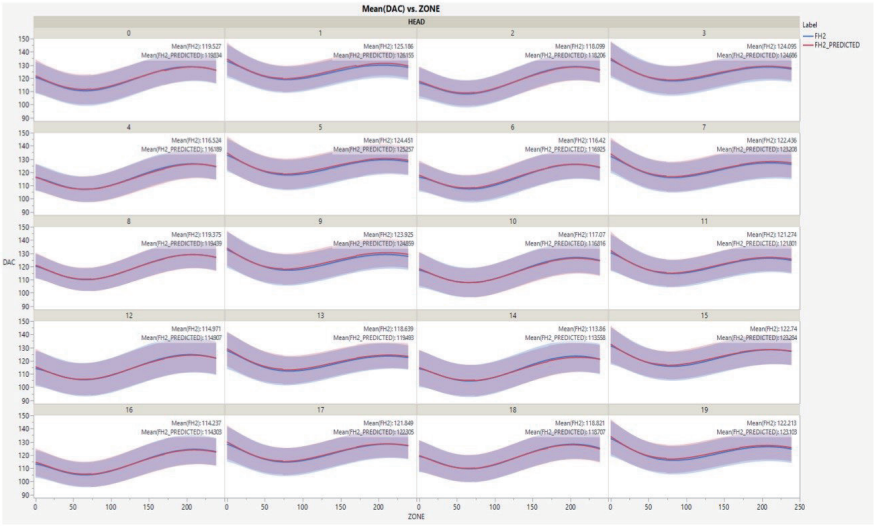

Fig. 14. (Color online) DAC profiles for each read/write head obtained from actual measurements and predictions of FH2 from the new HDD group.

4. Conclusions

We present an approach to FH measurement using the predictive power of a DNN based on PSO, termed as DNNpso. This method helps determine an appropriate and efficient number of nodes in hidden layers and is a novel approach to FH measurement that can be applied seamlessly to AI. The predictive capability significantly reduces the time required for FH measurement; therefore, it is expected to play a crucial role in streamlining the production of HDDs. The utilization of data from the source FH1 demonstrates the effectiveness of accuracy in predicting FH2 efficiently.

Acknowledgments

This research was made possible through the funding received from the School of Engineering, King Mongkut's Institute of Technology Ladkrabang for industrial purposes (grant number 2565-02-01-070).

References

1 H. Dakroub, M. C. Rao, and A. G. Sam: "Fly Height Measurement for A Disc Drive," US Patent: US6898034, Assignee: Seagate Technology LLC, Publication date on May 24, 2005 https://patents.google.com/patent/US6898034B2/en (accessed February 2023).
2 B. C. Schardt, E. Schreck, R. Sonnenfeld, Q. Haddock, and J.R. Haggis: IEEE Trans. Magn. **34** (1998) 1765. https://doi.org/10.1109/20.706699
3 V. J. Novotny: IEEE Trans. Magn. **33** (1997) 3115. https://doi.org/10.1109/20.617862
4 J. Y. Juang, T. Nakamura, B. Knigge, Y. Luo, W. C. Hsiao, K. Kuroki, F. Y. Huang, and P. Baumgart: IEEE Trans. Magn. **44** (2008) 3679. https://doi.org/10.1109/TMAG.2008.2002612

5 U. Boettcher, H. Li, R. A. de Callafon, and F. E. Talke: IEEE Trans. Magn. **47** (2011) 1823. https://doi.org/10.1109/TMAG.2011.2136328
6 W. Shi, D. Liu, X. Cheng, Y. Li, and Y. Zhao: IEEE Access **7** (2019) 104591. https://doi.org/10.1109/ACCESS.2019.2932266
7 F. E. Fernandes Junior, and G. G. Yen: Swarm Evol. Comput. **49** (2019) 62. https://doi.org/10.1016/j.swevo.2019.05.010
8 B. A. Garro and R. A. Vazquez: Comput. Intell. Neurosci. **2015** (2015) 369298. https://doi.org/10.1155/2015/369298
9 P. Konghuayrob and S. Kaitwanidvilai: Int. J. Innovative Comput., Inf. Control **13** (2017) 1777. https://doi.org/10.24507/ijicic.13.06.1777
10 T. Lawrence, L. Zhang, C. P. Lim, and E. J. Philips: IEEE Access **9** (2021) 14369. https://doi.org/10.1109/ACCESS.2021.3052489
11 J. Chen, W. Ding, X. M. Li, X. Xi, K. P. Ye, H. B. Wu, and R. X. Wu: IEEE Antennas Wirel. Propag. Lett. **20** (2021) 1993. https://doi.org/10.1109/LAWP.2021.3101703
12 Y. Gao, H. Liu, F. Niu, and Y. Tian: IEEE Access **11** (2023) 10366. https://doi.org/10.1109/ACCESS.2023.3240444
13 B. Lin, Y. Huang, J. Zhang, J. Hu, X. Chen, and J. Li: IEEE Trans. Ind. Inf. **16** (2019) 5456. https://doi.org/10.1109/TII.2019.2961237
14 X. Chen, J. Zhang, B. Lin, Z. Chen, K. Wolter, and G. Min: IEEE Trans. Parallel Distrib. Syst. **33** (2021) 683. https://doi.org/10.1109/TPDS.2021.3100298
15 A. Rajagopal, G. P. Joshi, A. Ramachandran, R. T. Subhalakshmi, M. Khari, S. Jha, K. Shankar, and J. You: IEEE Access **8** (2020) 135383. https://doi.org/10.1109/ACCESS.2020.3011502